AIP | Journal of Applied Physics

Three-dimensional optical analyses and optimizations of a vertical alignment color-filters-embedded liquid-crystal-on-silicon microdisplay

Baolong Zhang, Dan Li, Fengzhi Dai, Shifeng Yang, and Hoising Kwok

Citation: J. Appl. Phys. **110**, 063115 (2011); doi: 10.1063/1.3642967
View online: http://dx.doi.org/10.1063/1.3642967
View Table of Contents: http://jap.aip.org/resource/1/JAPIAU/v110/i6
Published by the American Institute of Physics.

Three-dimensional optical analyses and optimizations of a vertical alignment color-filters-embedded liquid-crystal-on-silicon microdisplay

Baolong Zhang,[1,a)] Dan Li,[1] Fengzhi Dai,[1] Shifeng Yang,[1] and Hoising Kwok[2]
[1]*College of Electronic Information and Automation, Tianjin University of Science and Technology, Tianjin 300222, People's Republic of China*
[2]*Center for Display Research, The Hong Kong University of Science and Technology, Clear Water Bay, Kowloon, Hong Kong, People's Republic of China*

(Received 25 May 2011; accepted 15 August 2011; published online 29 September 2011)

The process of vertical alignment (VA) mode color filter liquid crystal on silicon (CF-LCoS) microdisplay was developed. In order to minimize the fringing field effect in small color pixels, a three dimensional (3D) optical model was established and performed to analyze this VA mode CF-LCoS microdisplay. The simulated result was compared with the experimental data and they coincided well. Optimization of this breed of VA mode CF-LCoS microdisplay was proposed with optimal pretilt angle and pixel size. With the pretilt angle of 86 degrees and the pixel size of 15 μm, the color purity of the VA mode CF-LCoS microdisplay could attain more than 60% National Television Standards Committee (NTSC) level, and the contrast was larger than 400. © *2011 American Institute of Physics*. [doi:10.1063/1.3642967]

I. INTRODUCTION

Color filter liquid-crystal-on-silicon microdisplay (CF-LCoS) is a practical display technology that integrates color filters on silicon. We have developed the process, characterization, and three-dimensional (3D) optical model of this kind of CF-LCoS microdisplays[1–4] in mixed twist nematic (TN) mode.[5] For those microdisplays, the rubbed or photo-aligned methods[6] were used for the alignment process. As the experimental result, such microdisplays worked well for near-to-eye displays that had light illumination energy less than 8×10^6 lux. However, when such microdisplays were used for projections, the display performance degraded, since the light illumination energy exceeded 15×10^6 lux. Although the color filter has good stability against the high illumination, the alignment layer suffers from the ultraviolet part of the light. As a result, the contrast and color saturation of the display was accordingly degraded.

In this paper, the research on vertical aligned (VA) mode CF-LCoS microdisplays is reported. The use of silicon oxide as an inorganic alignment layer could improve the light stability of the microdisplays. Because of the normally black characteristics, the contrast for the CF-LCoS microdisplay in VA mode should be also improved.[7] In order to optimize the performance, we performed the three-dimensional (3D) optical analyses for VA mode CF-LCoS microdisplays.

II. PROCESS OF VA MODE CF-LCOS MICRODISPLAYS

The assembly process of the VA mode is more or less the same as that of the conventionally TN mode, except the alignment layer. Although, the special polyimide layers could also be applied on the silicon and glass substrate as the alignment layer for the VA mode,[8,9] the pretilt angles were limited, which resulted in the low response rate for the CF-LCoS microdisplays. On the other hand, they still had the light stability problem, since the polyimide-based alignment layer was a breed of organic material. As a result, the silicon oxide was widely used as the alignment layer of the LCoS microdisplays in VA mode.[10–15]

In this research work, the silicon oxide was also adopted as the alignment layer for the process of VA mode CF-LCoS microdisplay. The color filter array was prepared on the silicon substrate by the same process as reported in our previous works.[1,2] The thickness of the color filter array was 0.75 μm for all three colors. Then, a thin layer of silicon oxide was sputtered on the silicon substrate as the alignment layer with low temperature process. Thereafter, a CF-LCoS microdisplay of VA mode was assembled with a cell gap of 3 μm, and a Liquid Crystal (LC) mixture, MLC-6608 ($n_e = 1.5578$, $n_0 = 1.4748$, and $\Delta\varepsilon = -4.2$) from Merck, was filled into the cell for the assembly of the microdisplay.

The pretilt angle of the silicon oxide alignment layer could be adjusted by the direction of the sputtering process. With the tuning of the sputtering angle, a pretilt angle of 86° was formed on both the glass and silicon backplane. Thereafter, we emphasize on the establishment of a 3D optical model for this VA mode CF-LCOS microdisplay and its optimizations.

III. 3D OPTICAL MODEL

The 3D optical model of the VA mode was the extension of its counterpart of TN mode, as reported in our previous works.[3,4] It was divided into the following three steps: The 3D optical analysis started with a numerical calculation of liquid crystal (LC) director in rectangular mesh. In this step, 3D director configurations were calculated by simultaneously solving the 3D Poisson equation

$$\nabla[\vec{\varepsilon}(x,y,z)\nabla V(x,y,z)] = 0 \quad (1)$$

and continuum equation

a)Author to whom correspondence should be addressed. Electronic mail: eezbl@tust.edu.cn.

$$\gamma \frac{\partial n_i}{\partial t} = \frac{d}{d_j}\left[\frac{\partial (F_s - F_e)}{\partial\left(\frac{\partial n_i}{\partial j}\right)}\right] - \frac{\partial (F_s - F_e)}{\partial n_i}, \quad (2)$$

where γ is the rotational viscosity and F_s and F_e are the elastic and electrostatic energy density functions,[16] respectively. Periodic boundary conditions were applied on both the left and right edges, at which the director, potential, and their derivatives were continuous. Figure 1(a) shows the top view of the simulation structure. There were two pixels in the simulation structure, and each pixel included three sub-pixels of red, green, and blue. The sub-pixels were arranged in a delta shape and had a pitch of 10 μm by 7.5 μm with a pixel gap of 0.5 μm. A cross section of the simulation structure is also shown in Fig. 1(b). In this arrangement, the LC cell was driven in frame inversion, in which the green sub-pixel was 0 V, and the red and blue sub-pixels were 4 V. The thickness of the color filter array was 0.75 μm, and the LC cell gap was 3 μm in the simulation.

The common voltage on the top electrode was kept at a constant voltage of 5 V. As a result, the sub-pixel of 0 and 4 V produced a root-mean-squared voltage of 5 and 1 V, respectively, across the color filter and LC layers. For a fair comparison with the experimental data, the same LC mixture, MLC-6608 from Merck, was used for the simulation.

The simulated director distribution of the VA mode on the CF-LCoS structure is also shown in Fig. 1(b). With the homeotropic alignment, the LC molecules were aligned perpendicular to the surface of the substrate in off-state, as shown by the non-selected sub-pixels in Fig. 1(b). At this state, the LC layer introduced zero birefringence to the incident polarized light, and hence, a good dark state resulted through cross polarizers. It could ensure high contrast of the display. The LC mixtures used in the VA mode had a negative dielectric anisotropy. When an electric field was applied,

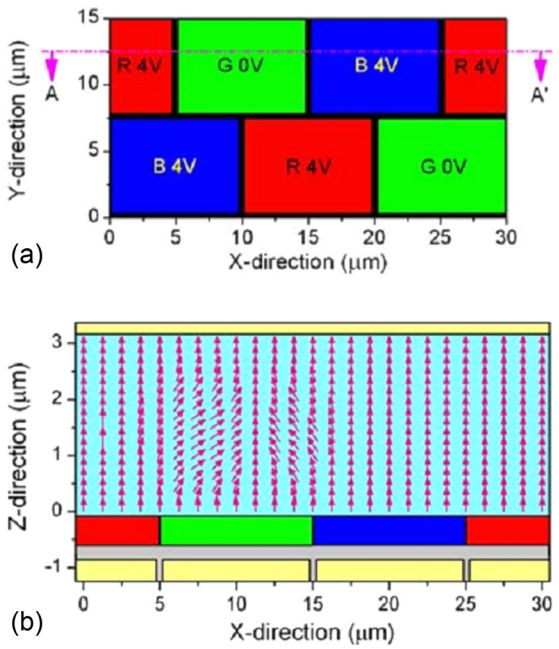

FIG. 1. (Color online) (a) Top and (b) cross section of the simulation structure.

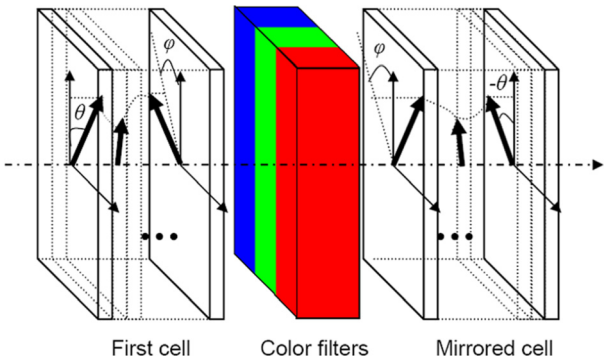

FIG. 2. (Color online) The optical reflectance model of the reflective color pixels of VA mode.

the LC molecules were lined up and parallel to the surface of the substrate, as shown by the selected sub-pixel in Fig. 1(b).

Thereafter, we calculated for optical reflectance of color pixels in the visible spectrum by extended Jones matrix.[17] We modeled the reflective color pixels by a transmittive LC cell, color filters, and a mirrored transmittive LC cell of the first one in series, as shown in Fig. 2. The LC cells were treated as a stack of uniaxial and isotropic media. The color filters were represented by absorptive and isotropic media. The optical reflectance was calculated as the ratio of output over input intensity. The overall optical behavior of the color LC cell with cross polarizers could be expressed as

$$\begin{bmatrix} E_{po} \\ E_{so} \end{bmatrix} = P_o \cdot M(-\theta, \emptyset, -\Delta\varphi) \cdot D_{CF\to LC} \cdot P_{CF} \cdot D_{LC\to CF} \cdot M(\theta, \emptyset, \Delta\varphi) \cdot P_i \cdot \begin{bmatrix} E_{pi} \\ E_{si} \end{bmatrix}, \quad (3)$$

where P_i and P_0 are matrix representations of the real input and output polarizers, E_{pi} and E_{si} are electric fields of the incident p and s vectors, and E_{po} and E_{so} are electric fields of the output **p** and **s** vectors, respectively. $M(-\theta_t\phi_t - \Delta\varphi)$ and $M(\theta_t\phi_t\Delta\varphi)$ represent the propagation matrices through the first and mirrored LC cells, respectively. In this work, a polarizing beam splitter with finite extinction ratio of 3000:1 and limited acceptance angle of $\pm 7^\circ$ was employed and studied. Then, the matrix representations of P_i and P_0 could be expressed as

$$P_i = \begin{pmatrix} 1 & 0 \\ 0 & 1/3000 \end{pmatrix} \quad (4)$$

$$\text{and, } P_o = \begin{pmatrix} 1/3000 & 0 \\ 0 & 1 \end{pmatrix}. \quad (5)$$

The reflectance of the color LC cell is, therefore,

$$R = \frac{|E_{so}|^2 + |E_{po}|^2}{|E_{si}|^2 + |E_{pi}|^2}. \quad (6)$$

The reflectance spectrum was then converted to the CIE 1931 color space[18] for color coordinates. We further expressed the optical reflectance in standard RGB[19] bitmap format

$$\begin{bmatrix} R_{sRGB} \\ G_{sRGB} \\ B_{sRGB} \end{bmatrix} = \begin{bmatrix} 3.2410 & -1.5374 & -0.4986 \\ -0.9692 & 1.8760 & 0.0416 \\ 0.0556 & -0.2040 & 1.0570 \end{bmatrix} \begin{bmatrix} X \\ Y \\ Z \end{bmatrix}_{D65}, \quad (7)$$

so we were able to visualize the color fringing effects among small color pixels.

With an attempt to verify the accuracy of this 3D optical model of the VA mode, the simulated spatial optical reflectance was compared with the observed optical reflectance of the CF-LCoS microdisplay sample prepared in Sec. II. Figure 3(a) shows the observed spatial optical reflectance of the VA mode CF-LCoS microdisplays. It should be noted that the sputtered oxide should produce an 86° pretilt angle on both the glass plate and color filter substrate. With the systematic comparisons, we found that the simulation result of the 86° pretilt angle, which was shown in Fig. 3(b), coincided with the experimental one very well.

IV. OPTIMIZATIONS

With this 3D optical analysis as a tool, we were able to locate the disclination lines and minimize the color fringing effect in VA mode CF-LCoS microdisplays, accordingly. In this section, the color purity and reflectivity of the pixel array were compared with respect to the pretilt angle and pixel size.

A. Pretilt angle

Pretilt angle is an important parameter to determine the performance of the VA mode CF-LCoS microdisplays. Contrast ratio, response time, color purity, and optical reflectance are all related to the pretilt angle.[20–22] Figure 4 shows the simulated spatial optical reflectance of the color pixel array,

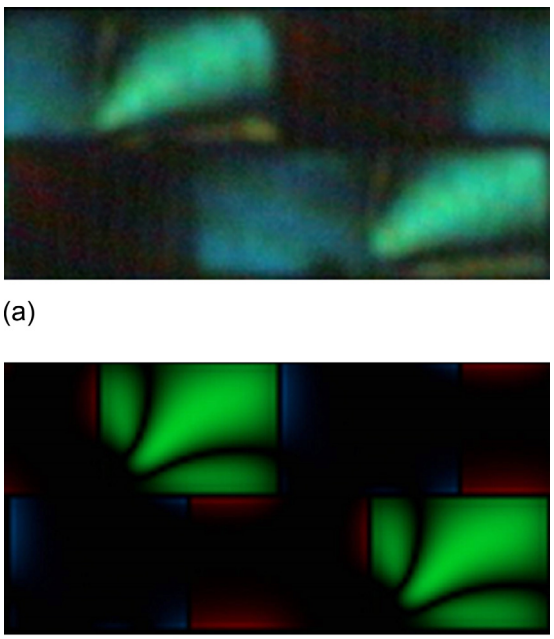

(a)

(b)

FIG. 3. (Color online) (a) Observed and (b) simulated spatial optical reflectance of the CF-LCoS microdisplays of VA mode.

which had a pixel pitch of 15 μm, and the pretilt angle was reduced from 90° to 80°. There were four symmetrical LC domains when the pretilt angle was 90°. At this angle, there was no preferable rotational direction for LC molecules when a voltage was applied. As a result, each quadrant has a symmetrical pattern, which was denoted as d1, d2, d3, and d4 and also shown in Fig. 4(a) for easier referring and descriptions later.

When the pretilt angle was reduced from 90° toward 80°, the center of the declination lines had the tendency to be moved toward the bottom-left corner of the ON pixel. This was due to the twist angle on the silicon substrate of the VA mode CF-LCoS microdisplay, which was −135° to the horizontal direction. When the pretilt angle was less than 90°, the LC director would have a preferable rotational direction toward the bottom-left corner of the pixel. As a result, domains d1, d3, and d4 were shrunk to a smaller size. On the contrary, domain d2 was enlarged.

When the pretilt angle was reduced to 86°, domains d2 and d3 were combined, and three domains in one sub-pixel resulted. When the pretilt angle was further reduced, the combined d2 and d3 domains were further increased and occupied more area of the ON pixel. As a result, optical reflectance of the ON pixel was increased.

While the optical reflectance of the ON pixel was increased due to a smaller pretilt angle, the leakage in the OFF pixel was also increased. The dark state in the off-pixels was degraded because of the residue birefringence, which is caused by the pretilt angle. This resulted in the light leakage in non-selected sub-pixels and degraded the color and contrast of the device at an 80° pretilt angle, which is clearly shown in Fig. 4(f).

Figure 5 shows the peak reflectivity and contrast ratio of the VA mode CF-LCoS microdisplays with respect to the pretilt angle. The peak reflectivity of the green image was increased from 4.52% to 8.43% when the pretilt angle was reduced from 90° to 80°. Similarly, the peak reflectivity of the red and blue images was increased from 3.79% to 7.86% and 5.49% to 8.62%, respectively, when the pretilt angle was reduced from 90° to 80°.

On the other hand, the contrast was dropped from 3×10^3 when the pretilt angle was 90° and rapidly to 1×10^3 when the pretilt angle was 88°. The contrast was continuously dropped to 2.5×10^2 when the pretilt angle was 84° and then to about 1.5×10^2 when the pretilt angle was 80° for the green image.

As the contrast was reduced at a lower pretilt angle, the color saturation of the display was also reduced. Figure 6 shows the color ordinates of the VA mode CF-LCoS microdisplays with respect to pretilt angle. The color purity was reduced from 66.8% NTSC level at a 90° pretilt angle to 62.5% at 86°, 58.4% at 84°, and 46.8% at an 80° pretilt angle.

It is hard to find an optimal pretilt angle for the VA mode CF-LCoS microdisplay, since a larger pretilt angle is favored for contrast, while a low pretilt angle is favored for optical reflectance. A compromise has to be made, and the 86° pretilt angle could be a good choice. At this pretilt angle, the color purity could attain more than 60% NTSC level with

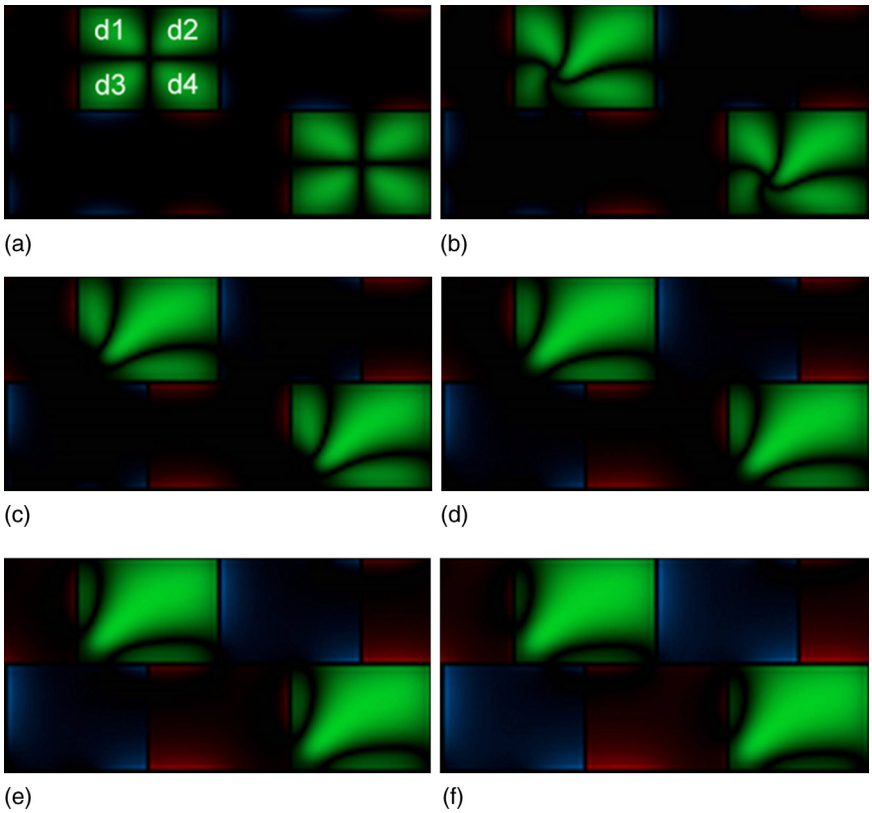

FIG. 4. (Color online) The evolution of simulated spatial optical reflectance of color pixel array with pretilt angle of (a) 90°, (b) 88°, (c) 86°, (d) 84°, (e) 82°, and (f) 80°.

a contrast larger than 400. The peak reflectivity of color images was reasonably high at 4.91%, 5.52% and 6.28%, respectively, for red, green, and blue colors.

B. Pixel size

Pixel size is another important parameter to determine the performance of the VA mode CF-LCoS microdisplays.[23–25] The relationship between the optical reflectance and color purity with respect to pixel size could also be analyzed by this 3D optical model. Figure 7 shows the spatial optical reflectance of the color pixel arrays, which had a pixel pitch of 12, 15, 18, and 21 μm, respectively. The pretilt angle was 86° and the cell gap was 3 μm in the simulation.

All these pixels had a similar pattern or LC domains, since the pretilt angle was the same. However, the percentage of the bright image in the ON pixel was increased with larger pixel size. As a result, the color purity was also increased with respect to the pixel size. It was found that the color coordinates of the green image were improved from (0.237, 0.607) at 12 μm, to (0.237, 0.610) at 15 μm, to (0.237, 0.613) at 18 μm, and to (0.238, 0.615) at 21 μm pixel. Similarly, the red and blue color purity was also increased slightly from (0.628, 0.300) and (0.134, 0.169) at 12 μm, to (0.636, 0.301) and (0.133, 0.170) at 15 μm, to (0.644, 0.302) and (0.133, 0.170) at 18 μm, and to (0.650, 0.303) and (0.132, 0.171) at the 21 μm pixel, respectively.

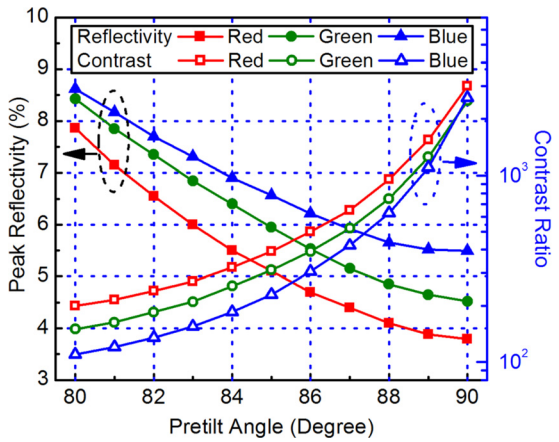

FIG. 5. (Color online) The optical reflectance and contrast of the VA mode CF-LCoS microdisplays with respect to pretilt angle.

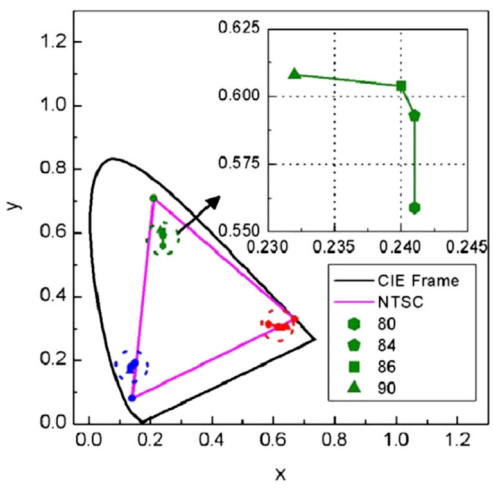

FIG. 6. (Color online) The color coordinates of the VA mode CF-LCoS microdisplays with respect to pretilt angle.

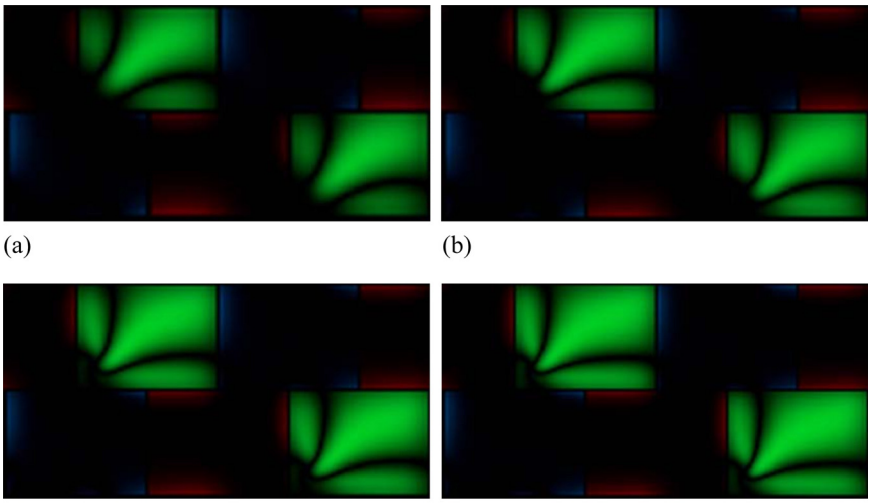

FIG. 7. (Color online) The spatial optical reflectance of color pixel arrays with pixel pitch of (a) 12, (b) 15, (c) 18, and (d) 21 μm.

The peak reflectivity of the color images was also increased with pixel size. It was found that the peak reflectivity of the green image was increased from 4.45% of the 12 μm to 5.52% of the 15 μm, to 6.37% of the 18 μm, and to 7.08% of the 21 μm pixel.

Similarly, the overall optical reflectance of red and blue is also increased from 3.86% and 5.18% of the 12 μm, to 4.91% and 6.28% of the 15 μm, to 5.80% and 7.11% of the 18 μm, and to 6.56% and 7.78% of the 21 μm pixel, respectively. It should be noted that the overall brightness of the pixel array were the same, since there was no fringing field when all the red, green, and blue pixels were turned on and off at the same voltage. The increase of the pixel size would raise the color saturation and individual color.

C. Thickness of color filters and LC cell gap

In addition to the pretilt angle and pixel size, the thickness of the color filters and cell gap of the LC cell could also affect the display performance of the VA mode CF-LCoS microdisplays. The dependence of the VA mode on these two parameters was also analyzed with this 3D optical model. It was found that these two parameters did not change the display performance of the VA mode CF-LCoS microdisplay as much as that of the pretilt angle and pixel size. As a result, the discussion of these two parameters on the VA mode CF-LCoS microdisplays was neglected in this paper. In short, a thicker color filter array could improve color saturation of the display, but a corresponding high driving voltage from the silicon backplane was required to maintain a good contrast of the VA LC cell.

V. CONCLUSIONS

In this paper, we developed the process of VA mode CF-LCoS microdisplay. The fringing field effect of this kind of microdisplay was analyzed by the 3D optical analysis tool. An experiment was performed to evaluate the simulation accuracy. The simulated optical reflectance agreed well with the experiment. How the dark disclination lines, which were generated by fringing field effect, affected the optical reflectance was discussed. In order to improve the optical efficiency, the dependences of overall optical reflectance on pretilt angle and pixel size were also analyzed. With optimal pretilt angle and pixel size, the overall optical reflectance was increased without sacrificing much contrast.

[1]H. C. Huang, B. L. Zhang, H. S. Kwok, P. W. Cheng, and Y. C. Chen, SID Int. Symp. Digest Tech. Papers **36**, 880 (2005).
[2]H. C. Huang, B. L. Zhang, H. J. Peng, H. S. Kwok, P. W. Cheng, and Y. C. Chen, J. Soc. Inf. Disp. **14**(5), 499 (2006).
[3]B. L. Zhang, H. J. Peng, H. C. Huang, and H. S. Kwok, SID Int. Symp. Digest Tech. Papers **36**, 1302 (2005).
[4]B. L. Zhang, H. S. Kwok, and H. C. Huang, J. Appl. Phys. **98**, 123103 (2005).
[5]S. T. Wu and C. S. Wu, Appl. Phys. Lett. **68**, 1455 (1996).
[6]B. L. Zhang, K. K. Li, V. G. Chigrinov, H. S. Kwok, and H. C. Huang, Jpn. J. Appl. Phys. **44**, 3983 (2005).
[7]S. Shimizu, Y. Ochi, A. Nakano, and M. Bone, SID Int. Symp. Digest Tech. Papers **35**, 72 (2004).
[8]J. Kim, S. Kim, K. Park, and T. Kim, SID Int. Symp. Digest Tech. Papers **32**, 806 (2001).
[9]V. Konovalov, V. Chigrinov, H. S. Kwok, H. Takada, and H. Takatsu, Jpn. J. Appl. Phys. **43**, 261 (2004).
[10]Microdisplay Rep. **6**, 1 (2003).
[11]R. D. Sterling and W. P. Bleha, Int. Disp. Works **4**, 809 (1997).
[12]A. Nakano, A. Honma, S. Nakagaki, and K. Doi, Proc. SPIE Int. Soc. Opt. Eng. **3296**, 100 (1998).
[13]T. Katayama, H. Natsuhori, T. Moroboshi, M. Yoshimura, and M. Hayakawa, SID Int. Symp. Digest Tech. Papers **32**, 976 (2001).
[14]C. Dieter, V. D. Geert, V. D. Steen, D. S. Herbert, and V. C. André, Conf. Rec. Int. Disp. Res. Conf. **22**, 1083 (2002).
[15]C. H. Wen, S. Gauza, and S. T. Wu, J. Soc. Inf. Disp. **13**(9), 805 (2005).
[16]S. Dickmann, J. Eschler, O. Cossalter, and D. Mlynski, SID Int. Symp. Digest Tech. Papers **22**, 638 (1993).
[17]C. Gu and P. Yeh, J. Opt. Soc. Am. A **10**, 966 (1993).
[18]G. Wyszecki and W. S. Stiles, *Color Science: Concepts and Methods, Quantitative Data and Formulae* (Wiley, New York, 1982), Chap. 3.
[19]See http://www.color.org/sRGB.html for information about sRGB standard.
[20]H. D. Smet, D. Cuypers, A. V. Calster, J. V. D. Steen, and G. V. Doorslaer, Displays **23**, 89 (2002).
[21]A. V. Calster and D. Cuypers, Proc. SPIE **3954**, 112 (2000).
[22]D. Cuypers, H. D. Smet, and A. V. Calster, SID Int. Symp. Digest Tech. Papers **36**, 1298 (2005).
[23]P. J. M. Vanbrabant, J. Beeckman, K. Neyts, R. James, and F. A. Fernandez, J. Disp. Technol. **7**, 156 (2011).
[24]D. Armitage, I. Underwood, S. T. Wu, *Introduction to Microdisplays* (Wiley, New York, 2006).
[25]K.-H. Fan-Chiang, S.-T. Wu, and S.-H. Chen, J. Disp. Technol. **1**, 304 (2005).